JOURNAL OF AIRCRAFT
Vol. 47, No. 4, July–August 2010

Engineering Notes

Experimental Investigation of Double-Hinged Vortex Flap Configurations

Kenneth Toro,* Thomas Nix,* and Lance W. Traub†
Embry-Riddle Aeronautical University, Prescott, Arizona 86301

DOI: 10.2514/1.46691

Introduction

DELTA wings are poor lift generators. An often-employed design approach to ameliorate the low lift production is to sharpen the wing's leading edge. A consequence of the enforced flow separation is the formation of leading-edge vortices. The vortices induce high surface velocities over the wing and may significantly augment lift, especially as the delta becomes more slender [1]. Leading-edge flaps (formed by downward rotation of a segment of the wing's leading edge) may be used to lessen the performance loss by recovering thrust from the vortices by positioning them over wing elements with a forward-facing area: so-called leading-edge vortex flaps (LEVFs) [2].

Studies of vortex flaps (VFs) have shown the concept to be effective [2,3]; however, their performance is constrained by the characteristics of the leading-edge vortices with incidence. The vortices expand in size and migrate inboard off the flap. As a result, the flaps lose effectiveness. A study by Rinoie and Stollery [3] showed that the maximum lift-to-drag ratio L/D for the 60 and 70 deg delta wings they tested with vortex flaps coincided with smooth flow onto the flap with no separation. As a result, increasing wing incidence requires larger flap deflections to maintain maximized L/D values. Deflecting the flap reduces lift for a given geometric angle of attack as the vortex strength is reduced, as well as to a lesser extent, the attached flow lift [4]. An additional byproduct of flap deflection is a moderate increase in the minimum-drag coefficient. As a result, the initial L/D is attenuated, but may increase significantly beyond that of the sharp planar delta for moderate to high lift coefficients. An attempt to reduce the drag penalty as well as limit the expansion of the vortex off the flaps was documented by Rao [5]. Various flap configurations were investigated, variants including constant length and segmented configurations. The segmented flaps generated two smaller distinct leading-edge vortices so as to minimize vortex spillage. Rao's results suggested that generating multiple leading-edge vortices was effective in delaying vortex spillage and thus suction loss from the flap.

Generally, experimental observation has indicated that the leading-edge vortices on a planar delta lie along a trajectory of approximately 70% of the local semispan [6]. It may be feasible to design a vortex flap that is located further inboard, such that the flap hingeline runs along a ray of approximately 65% semispan. To limit the flap size, a tab may be employed, where the outer wing surface is inclined so as to be parallel to the inner wing section (see Fig. 1). A small tab was evaluated by Hoffler and Rao [7]; some of their designs resulted in the tab having a rearward inclination such that vortex formation over the tab would contribute additional drag. Other tabbed configurations that were tested were not deemed as successful [7].

In this paper, so-called double-hinged vortex flaps (HVF) are evaluated, where the configuration consists of a planar inboard portion, a vortex flap and a planar outboard panel. HVFs may reduce vortex loss with incidence (as its hingeline orientation is closer to the *natural* vortex trajectory, i.e., the flap is located further inboard), the minimum-drag penalty and structural complication. The undeflected outboard panel of the HVF may also augment the strength of the primary vortex compared with a conventional LEVF, where the effective leading-edge incidence is diminished. The proposed design would mitigate against a movable flap; the wing configuration would be fixed. The basis of comparison of the flaps in this study is different from that of Hoffler and Rao [7]. In the present study the flap area is conserved for a given flap area ratio, and does not include the area of the outboard panel (or tab). The configuration and size of the outboard panels are also conceptually different from those in [7], where the tabs were approximately constant chord and were not an integral part of the wing design, but an add-on. A low-speed wind-tunnel investigation was conducted to evaluate the concept, characterized through force-balance, pressure measurement, surface flow visualization, and vortex burst trajectories.

Equipment and Procedure

In the present implementation, the projected planform of the wing is conserved and is that of a 65-deg-sweep delta wing. LEVF and HVF flap area ratios of 6 and 12% were evaluated (this area ratio is defined as the actual flap area: i.e., the area when viewed normal to the surface, divided by the total projected wing area). The force-balance wings were sheared and bent from a 1/16 in. aluminum plate. Reflection plane models were used. The chord length c of the wings was 8 in. (203 mm). The flap geometries evaluated and presented are shown in Fig. 1. The flap angle was 30 deg. This angle was selected as an effective performance compromise [3]. The hingeline sweep angles for the HVF was selected so as to place the flap just inboard of the often-observed vortex trajectory (along a ray at approximately 65% semispan for the tapered HVF and for the constant-chord HVF at the midchord location: i.e., the flap hinge intersects a line parallel to the leading edge at a point 65% of the semispan at the midchord position). While the camber caused by the flaps would alter this trajectory, it *may* be expected that the vortices trajectories would not be significantly altered. Data comparison indicated that the 12%-area-ratio constant-chord flaps were the most effective. Consequently, presented data are for these configurations only.

Wind-tunnel tests were conducted in Embry-Riddle University's 1 by 1 ft open-return facility. This wind tunnel has a measured turbulence intensity of 0.5% and jet uniformity within 1% in the core. The wall boundary layer is approximately 5 mm thick. Force measurements were taken using a low-range platform balance. The balance has a maximum range of 43 N and a demonstrated accuracy, resolution and repeatability of 0.0098 N. Angle setting ability is within 0.1 deg. The Reynolds number, based on the root chord was 400,000. Three wings, representing the planar delta, and the most effective vortex flap configurations (HVF and LEVF with 12% constant-chord flaps) were pressure-tapped. Fifteen tappings were distributed spanwise (y) at a 70% chordwise location. Tapping locations are shown in Fig. 1. The tubing had an internal diameter of

Received 10 August 2009; revision received 7 April 2010; accepted for publication 9 April 2010.

*Undergraduate Student, Aerospace and Mechanical Engineering Department.

†Associate Professor, Aerospace and Mechanical Engineering Department. Member AIAA.

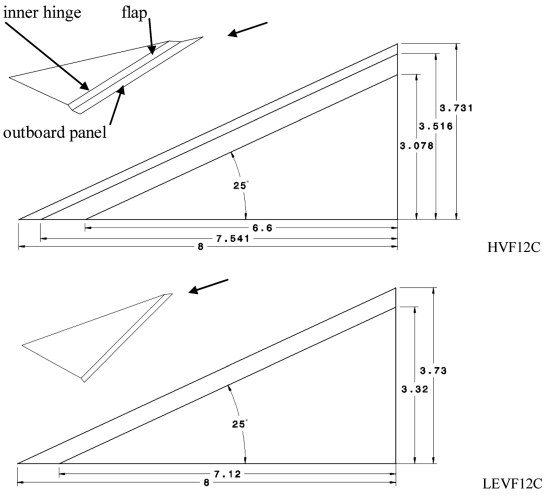

Spanwise Pressure Port Locations (s = local wing span)

2y/s	0.06	0.12	0.18	0.24	0.30	0.37	0.43	0.49	0.55	0.61	0.67	0.73	0.79	0.85	0.91	0.98

Fig. 1 Model geometry and pressure port locations (dimensions in inches).

approximately 0.3 mm. Pressures were measured using a 30-channel electronic pressure scanner. The pressure transducer outputs were digitized using a 32-channel 16-bit 250 kHz sampling rate National Instruments external Universal Serial Bus analog-to-digital converter board. All presented pressures are the average of 1000 readings. The tunnel freestream velocity was measured using a FlowKinetics^{TM} LLC FKT 2DP1A-C meter. Meter accuracy is specified by the manufacturer as better than 0.1%. As the tests are essentially comparative, no corrections for wall effects were applied.

Surface flow visualization was performed at AOA = 10 and 20 deg using a mixture of titanium dioxide, paraffin, linseed oil, and oleic acid. Vortex burst trajectories were recorded in a 5 by 12 in. water tunnel using rapid-prototyped acrylonitrile butadiene styrene models. Model chord was 122 mm. Dye constituted of dilute food coloring was injected near the apex so as to best elucidate the core. The burst location was identified as that at the beginning of the often-observed spiral or bubble structure, seen along the vortex core at the onset of bursting. Although the Reynolds number is considerably lower than in the wind-tunnel experiments, the essentially inviscid nature of breakdown is well documented [6].

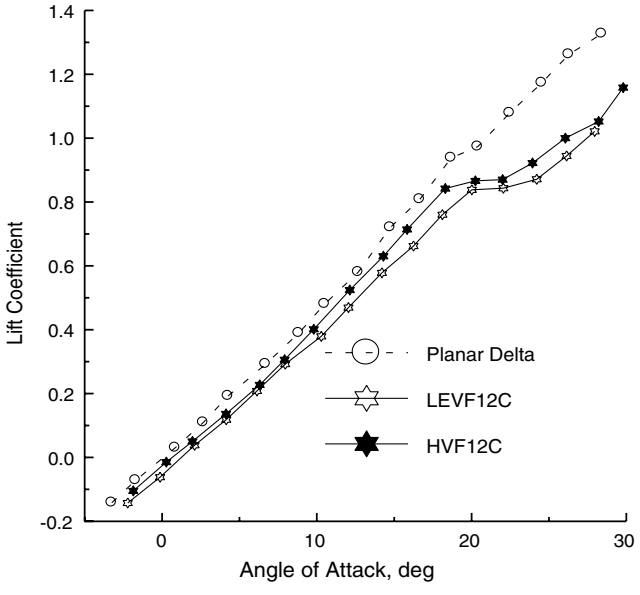

Fig. 2 Effect of VF geometry on measured lift coefficient.

Results and Discussion

Figure 2 presents the effect of the flap geometry on the measured lift coefficient. The VFs show a moderate positive zero-lift angle shift compared with the planar wing. Examination indicates that the conventional LEVF shows a larger loss of lift than the HVF flap. At high incidence, the VFs indicate a loss of lift compared with the planar wing. The form of the lift curves shows a nonlinear development for the planar and HVF wing. This is not evident for the LEFV and is suggestive of suppression or weakening of its leading-edge vortex. None of the flap configurations appear to have a significant impact on the minimum-drag coefficient (see Fig. 3a, bottom inset). For lift coefficients greater than 0.2 and less than 0.75, the VF variants show drag reduction compared with the planar wing. Also included in Fig. 3a is an estimate of the drag coefficient assuming full leading-edge suction, i.e., elliptic loading ($C_{D\min} + C_L^2/\pi\mathrm{AR}$), where C_L and $C_{D\min}$ are the lift and minimum-drag coefficient, respectively. For the estimate, the minimum-drag coefficient of the planar wing was used. As may be seen, the VF configurations are capable of achieving full suction at low lift coefficients although the LEVF displays full suction to higher lift than the HVF.

The lift-to-drag ratio is displayed in Fig. 3b. An estimate of the lift-to-drag ratio with full suction is also presented for reference. As may be surmised from the drag polars, the VF configurations match the full suction lift-to-drag ratio for low lift coefficients. At these conditions, flow visualization (shown later) suggests that the flow is

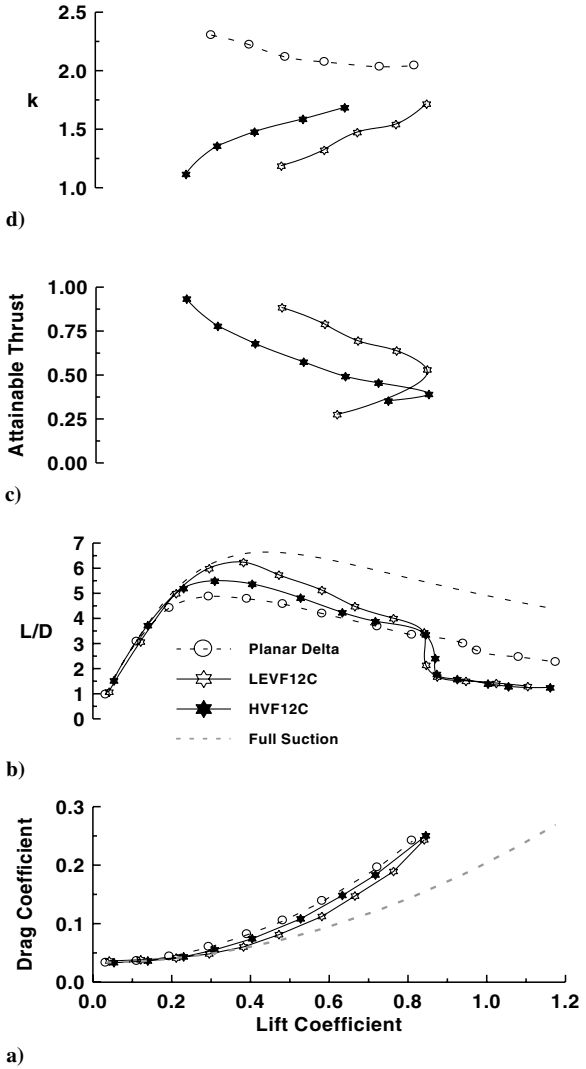

Fig. 3 Effect of VFs on drag-based performance characteristics: a) drag coefficient, b) L/D ratio, c) attainable thrust, and d) efficiency factor k.

essentially attached with little discernible evidence of vortex formation. The HVF12C configuration shows degraded performance compared with the LEVF12C, but a significant improvement compared with the planar wing. Figure 3c presents an estimate of the attainable leading-edge thrust, which may be interpreted as the ability of the flaps to develop a streamwise axial force that opposes drag. The attainable leading-edge thrust is presented. The attained thrust C_A is defined as

$$C_A = \frac{(C_L \sin\alpha - (C_D - C_{D\min})\cos\alpha)}{C_L \sin\alpha - (C_L^2/\pi\mathrm{AR})\cos\alpha} \tag{1}$$

and is the ratio of the measured thrust to that with 100% leading-edge suction (i.e., that with elliptic loading). The LEVF is seen to develop higher thrust levels than the HVF. Attainable thrust is also seen to diminish with increasing lift coefficient as a consequence of the corresponding drag rise. Figure 3d presents the wing efficiency, k, calculated as

$$k = \left(\frac{C_D - C_{D\min}}{C_L^2}\right)\pi\mathrm{AR} \tag{2}$$

For this relation, an improvement in efficiency is indicated by k tending toward 1, where unity represents elliptic loading. As may be seen, for the planar wing, efficiency increases with lift coefficient, due to increasing lift from the vortex sheets (in this instance $k = [\tan(\mathrm{AOA})/C_L]\pi\mathrm{AR}$). This tendency is not evident for the VF configurations, presumably due to their attenuation of nonlinear lift. However, in almost all cases, the VFs improve efficiency significantly compared with the planar wing. The 12% constant-chord LEVF demonstrated the highest efficiency of the tested wings.

A summary of measured upper surface pressure traces are shown in Fig. 4 for angles of attack (AOA) of 12, 16, and 20 deg. The spanwise row of tappings were located at 70% chord for all geometries. Note that the LEVF extent runs from the designated LEVF hingeline to the local wing semispan, $s/2$. At an angle of attack of 12 deg, the peak suction levels are similar for the three configurations. The planar delta shows evidence of a laminar secondary separation outboard of the primary suction peak [8]. Compared with the planar wing, the VFs vortex trajectories are closer to the leading edge. Also evident is that the LEVFs suction peak is narrower than the other two wing geometries, which could indicate a smaller primary vortex or closer wing proximity. However, it is suggested (as will be seen later) that vortex formation at this AOA may be suppressed, and the trace is that of attached flow (LEVF). Additionally, most of the upper surface suction for the LEVF and HVF (with some inboard spillage) at this incidence and location is concentrated on the flap. An increase of incidence to 16 deg still indicates similar peak suction values for the configurations. The suction footprint for the wing with a LEVF is seen to have expanded and moved inboard. The HVFs footprint has also moved inboard, but not necessarily expanded. Both VFs are seen to have lost flap suction due to the migration. The planar and HVF traces also suggest that their secondary vortices are turbulent [8] at this incidence. At an angle of attack of 20 deg the HVF has lost significant peak suction compared with the other wings. The HFV vortex trajectory has

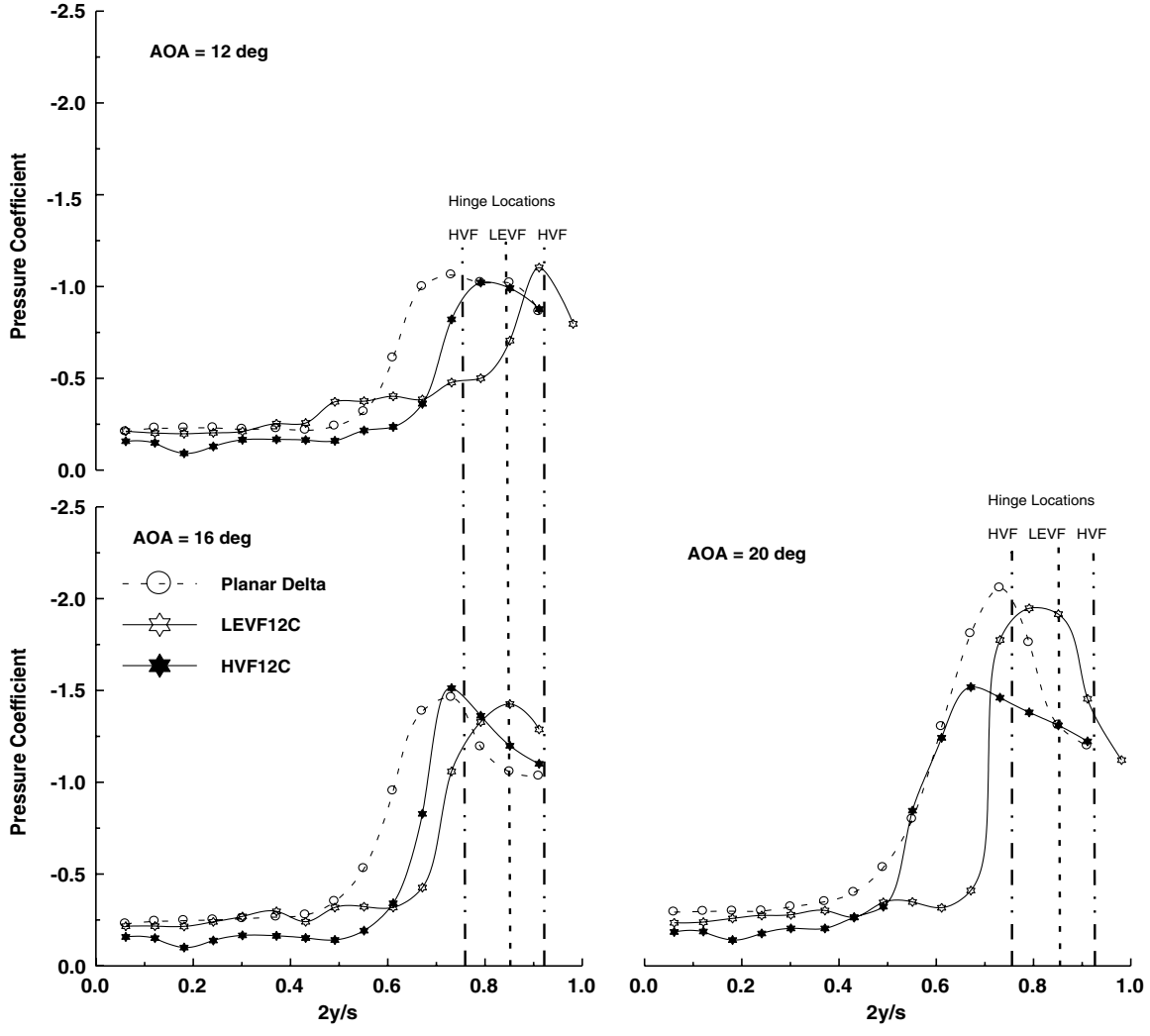

Fig. 4 Effect of leading edge and hinge vortex flaps on measured spanwise pressure coefficient.

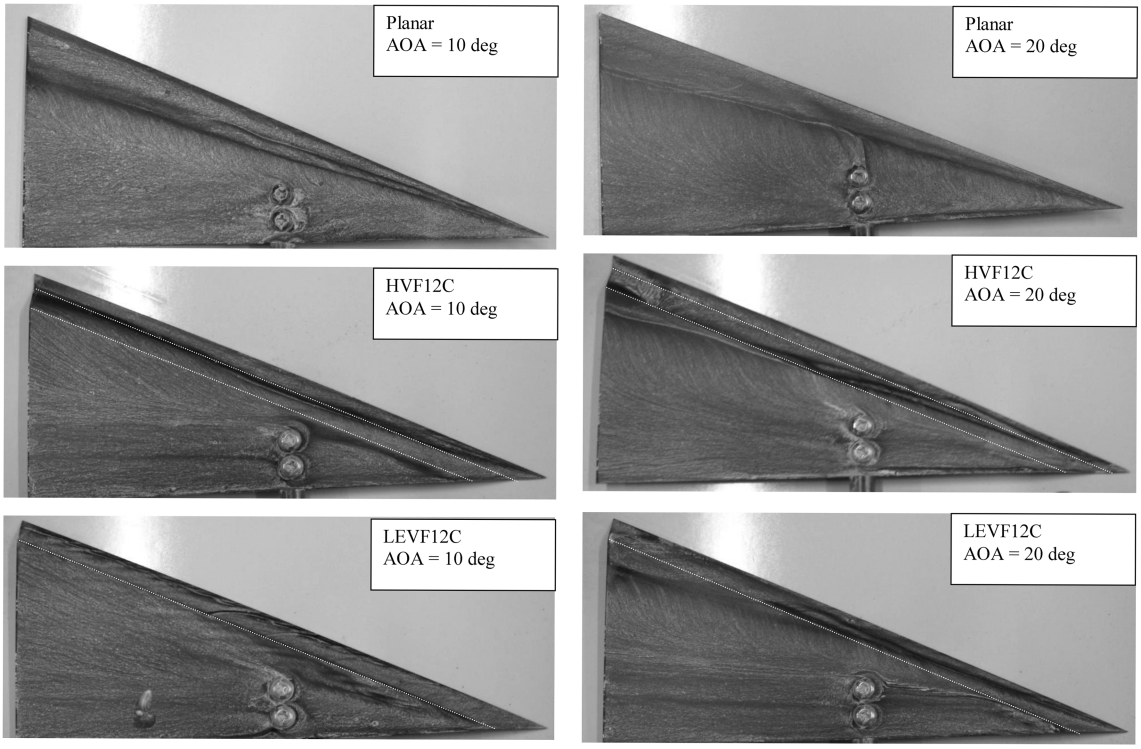

Fig. 5 Surface skin-friction traces for a) AOA = 10 deg and b) AOA = 20 deg

continued to migrate inboard, with a surface signature that is suggestive of vortex breakdown. The vortex trajectory for the LEVF also shows a moderate inboard movement.

Water-tunnel measurement indicated that the VFs tend to delay the onset and forward progression of vortex breakdown compared with the planar delta wing. This may be due to the flap weakening the leading-edge vortices (specifically, the vorticity forming the core), in a manner similar to a drooped leading edge [9]. The flaps weaken the vortices [9] and thus delay the incidence at which the critical swirl angle is reached.

Figure 5 presents a summary of surface skin-friction patterns rendered using titanium dioxide at 10 and 20 deg incidence. White dotted lines have been drawn onto the upper wing surfaces to aid in identification of the flap hinge locations. Figure 5a shows weak sidewash for the HVF configuration over the aft wing portions and a vortex trajectory inboard of the flap. The vortex trace over the aft wing section indicates capture by the flap. Secondary and tertiary separation lines are visible on the outboard wing panel/flap junction. The LEVF geometry shows suppression of vortex formation over the model. Considering this geometry, the angle of attack of a section normal to the wings leading edge is approximately the geometric angle of attack divided by the cosine of the leading-edge sweep angle. Consequently, for this incidence, the normal angle is 24 deg. However, the leading-edge flap angle reduces this to a geometric angle of -6 deg. While circulation induces a net upwash, the net inflow angle is small enough so that separation is minimized. The planar delta shows classical vortex formation with a well-defined primary vortex and secondary separation lines. The inclination of the sidewash lines is greater than the VF models, suggesting greater vortex strength and/or closer wing–vortex proximity.

Figure 5b shows skin-friction patterns at AOA $= 20$ deg. The HVF configuration shows vortex trajectories inboard of the flap and hingeline induced separation. The LEVF show suppression or weakening of the leading-edge vortex near the apex (with defined sidewash evident from approximately 30% aft). The secondary separation line(s) extending from the apex to approximately 70% of the chord on the LEVF12C does suggest primary vortex formation, even if weak in strength. The planar delta at AOA $= 20$ deg shows a well-defined pattern evolution from that seen at 10 deg AOA. The effect of incidence is indicated by an inboard movement of the primary attachment line commensurate with an increase of vortex size. The secondary separation lines are also seen to terminate at approximately 60% of the chord, potentially due to dissipation/bursting or lift off of these vortices.

Conclusions

A low-speed wind-tunnel investigation was undertaken to evaluate the effect of double-hinged vortex flaps on a 65-deg-sweep delta wing. These flaps are located further inboard than traditional leading-edge vortex flaps and consist of two panels: the inner, which is the flap, and the outer, which is orientated similarly to the inboard wing section (i.e., it is planar). The study examined the ability of these flaps to enhance performance by reducing vortex spillage at incidence. Two flap configurations were evaluated; one with a constant-chord outboard panel and the other with a triangular shaped outboard panel. Similarly configured leading-edge vortex flaps were also evaluated. A flap angle of 30 deg was used in all tests, which were run at $Re = 400,000$. Force balance, pressure measurement, and surface flow visualization results indicated that leading-edge vortex flaps were generally more effective than the double-hinged configurations evaluated. For both flaps designs, hinged or leading edge, the constant-chord geometry was seen to provide better performance. Peak lift-to-drag ratio also appeared to coincide with smooth onflow over the LEVF with little or no separation.

References

[1] Wentz, W. H., Jr., and Kohlman, D. L., "Vortex Breakdown on Slender Sharp-Edged Wings," *Journal of Aircraft*, Vol. 8, No. 3, 1971, pp. 156–161.
doi:10.2514/3.44247

[2] Lamar, J. E., and Campbell, J. F., "Vortex Flaps—Advanced Control Devices for Supercruise Fighters," *Aerospace America*, Jan. 1984, pp. 95–99.

[3] Rinoie, K., and Stollery, J. L., "Experimental Studies of Vortex Flaps

and Vortex Plates," *Journal of Aircraft*, Vol. 31, No. 2, 1994, pp. 322–329.
doi:10.2514/3.46490

[4] Oh, S., and Tavella, D., "Analysis of a Delta Wing with Leading-Edge Flaps," *Journal of Aircraft*, Vol. 24, No. 6, 1987, pp. 353–354.

[5] Rao, D. M., "An Exploratory Study of Area-Efficient Vortex Flap Concepts," *Journal of Aircraft*, Vol. 20, No. 12, 1983, pp. 1062–1067.
doi:10.2514/3.48213

[6] Traub, L. W., "Effects of Spanwise Camber on Delta Wing Aerodynamics: An Experimental and Theoretical Investigation," Ph.D. Dissertation, Aerospace Engineering Department, Texas A&M Univ., College Station, TX, May 1999.

[7] Hoffler, K. D., and Rao, D. M., "An Investigation of the Tabbed Vortex Flap," *Journal of Aircraft*, Vol. 22, No. 6, 1985, pp. 490–497.
doi:10.2514/3.45154

[8] Hummel, D., "On the Vortex Formation over a Slender Wing at Large Angles of Incidence," *High Angle of Attack Aerodynamics*, AGARD, CP-247, Jan. 1979.

[9] Lowson, M. V., and Riley, A. J., "Vortex Breakdown Control by Delta Wing Geometry," *Journal of Aircraft*, Vol. 32, No. 4, 1995, pp. 832–838.
doi:10.2514/3.46798